EPJ Web of Conferences **62**, 08001 (2013)
DOI: 10.1051/epjconf/20136208001
© Owned by the authors, published by EDP Sciences, 2013

Towards high accurate neutron-induced fission cross sections of ^{240,242}Pu: Spontaneous fission half-lives

P. Salvador-Castiñeira[1,2,a], T. Bryś[1], R. Eykens[1], F.-J. Hambsch[1,b], A. Moens[1], S. Oberstedt[1], C. Pretel[2], G. Sibbens[1], D. Vanleeuw[1], and M. Vidali[1]

[1] European Commission, Joint Research Centre, Institute for Reference Materials and Measurements (JRC-IRMM), Retieseweg 111, 2440 Geel, Belgium
[2] Institute of Energy Technologies, Technical University of Catalonia, Avda. Diagonal 647, 08028 Barcelona, Spain

Abstract. Fast spectrum neutron-induced fission cross sections of transuranic isotopes are being of special demand in order to provide accurate data for the new GEN-IV nuclear power plants. To minimize the uncertainties on these measurements accurate data on spontaneous fission half-lives and detector efficiencies are a key point. High α-active actinides need special attention since the misinterpretation of detector signals can lead to low efficiency values or underestimation in fission fragment detection. In that context, ^{240,242}Pu isotopes have been studied by means of a Twin Frisch-Grid Ionization Chamber (TFGIC) for measurements of their neutron-induced fission cross section. Gases with different drift velocities have been used, namely P10 and CH_4. The detector efficiencies for both samples have been determined and improved spontaneous fission half-life values were obtained.

1. Introduction

In a recent assessment of target accuracies and uncertainties the NEA highlighted the need for improved nuclear data to be used in model calculations for innovative reactor systems (GEN-IV) [1]. The neutron-induced fission cross sections of ^{240,242}Pu have been identified in this study as of highest priority for fast spectrum reactors. Their target uncertainties are very stringent and are requested to be lower than 5% in both cases from current uncertainties of 6% for ^{240}Pu and 20% for ^{242}Pu.

In the frame of the ANDES collaboration (Accurate Nuclear Data for nuclear Energy Sustainability) several actinides are being under study, among them ^{240,242}Pu. JRC-IRMM has been strongly involved in these measurements and has applied the new digital data acquisition techniques for cross section measurements. Using digital electronics and storing the full waveform opens up new analysis possibilities not available using regular analogue electronics.

[a] e-mail: paula.salvador-castineira@ec.europa.eu
[b] e-mail: franz-josef.hambsch@ec.europa.eu

This is an Open Access article distributed under the terms of the Creative Commons Attribution License 2.0, which permits unrestricted use, distribution, and reproduction in any medium, provided the original work is properly cited.

Article available at http://www.epj-conferences.org or http://dx.doi.org/10.1051/epjconf/20136208001

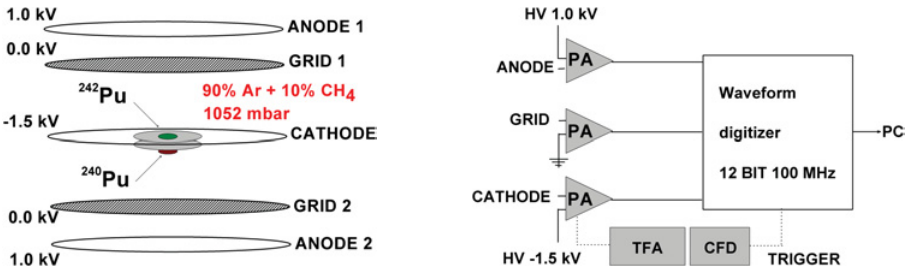

Figure 1. Schematic drawing of a Twin-Frisch Grid Ionization Chamber (TFGIC) with the two samples inside (left) and a scheme of the electronics for one chamber side (right).

Table 1. Main characteristics of the ^{240,242}Pu samples [2]. All the uncertainties have a coverage factor $k = 1$, but the sample purity has a coverage factor $k = 2$.

	^{240}Pu	^{242}Pu
Method	electrodeposition	electrodeposition
Chemical composition	$Pu(OH)_4$	$Pu(OH)_4$
Total areal density ($\mu g/cm^2$)	16.9 (0.4%)	122 (0.9%)
Backing	aluminium	aluminium
Areal density ($\mu g/cm^2$)	13.19 (0.4%)	95.3 (0.8%)
α-activity (MBq)	0.780 (0.4%)	0.0984 (0.3%)
Purity	99.8915(*18*)%	99.96518(*45*)%

In the present work we will focus on the determination of the detector efficiency and the spontaneous fission half-life, important ingredients in the final fission cross section determination, which will be subject of a forthcoming paper.

2. Experimental setup

A Twin Frisch-Grid Ionization Chamber (TFGIC) has been chosen as fission fragment detector due to its radiation resistance and a $2 \times 2\pi$ solid angle coverage. A schematic representation of the setup is presented in Figure 1. The two samples were placed in a back-to-back geometry on the common cathode. The TFGIC was filled with P10 (90% Ar + 10% CH_4) as counting gas at a pressure of 1052 mbar with a constant flow of ≈ 50 ml/min. The cathode-grid distance was 31 mm to fully stop the fission fragments (FF) and the grid-anode distance was 6 mm. Grids and anodes were connected to charge sensitive preamplifiers (PA) and then directly to a 12 bit 100 MHz Waveform Digitizer (WFD). The cathode signal was split after a current sensitive PA: one PA output was fed directly into the WFD and the second output was further treated and used as a global trigger to all WFD boards. All the samples used in this experiment were produced by the target preparation group at JRC-IRMM. A brief description of the ^{240,242}Pu samples is presented in Table 1 [2]. By assuming that the Pu deposits are hydroxide in the form of $Pu(OH)_4$, it is possible to calculate the total areal density of the deposit using the Pu areal density measured.

3. Data acquisition and treatment

3.1 α pile-up correction

One of the main challenges of this experiment is the high α-activity of the samples, specially that of ^{240}Pu. Digital electronics enables optimizing the analysis of individual signals and to perform α pile-up correction.

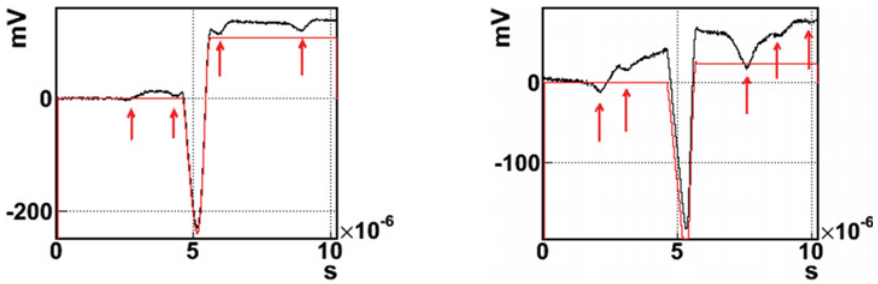

(a) Grid signal ^{242}Pu (0.1 MBq) (b) Grid signal ^{240}Pu (0.8 MBq)

Figure 2. Typical grid signals for ^{240,242}Pu. Black traces represent the raw signals as they are recorded; the red arrows point to possible α particle pile-ups; the red trace is the signal after α pile-up rejection.

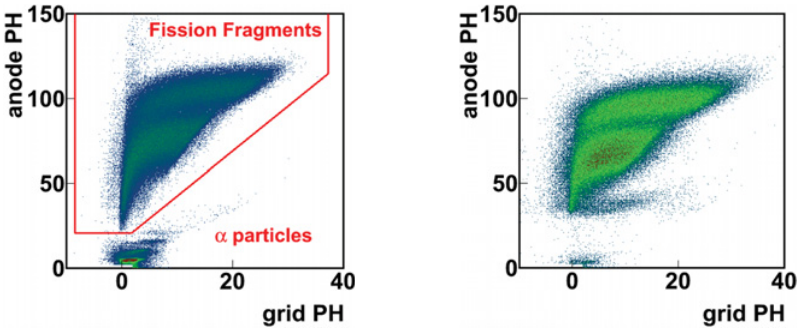

(a) ^{242}Pu (b) ^{240}Pu

Figure 3. Grid PH versus anode PH for the two isotopes. In the left picture one can see the distinction between α particles and FF.

Figure 2 presents typical grid signals for the two isotopes. In black the original signal is shown (the arrows show possible α pile-up signals), while the red one is after α pile-up rejection.

3.2 Efficiency determination – sample loss

Although the TFGIC has a nearly $2 \times 2\pi$ efficiency, our samples are not an infinite thin layer. Therefore, FFs emitted at increasing angles might be fully stopped inside the sample, preventing us from detecting them. The quantification of the sample loss is, thus, a quality check of the performance of this experiment and can provide valuable information on how to analyze data obtained with high α-active samples.

3.2.1 Angle determination

The FFs in spontaneous fission (SF) are emitted isotropically. By determining the angular distribution of the FF for each sample one should be able to account for the sample loss comparing the distribution measured with an ideal distribution, as presented in Ref. [3]. The grid signal has been used to determine the angular information according to Ref. [4]. Figure 3 presents the 2D representation of the grid pulse height (PH) versus the anode PH.

In the grid method, after excluding the α particle signals with a region of interest, it is possible to determine the cosinus distribution by knowing that fragments emitted at 90° will have a grid PH close to 0, while the maximum values for the Grid (after projecting the distribution onto the anode axis)

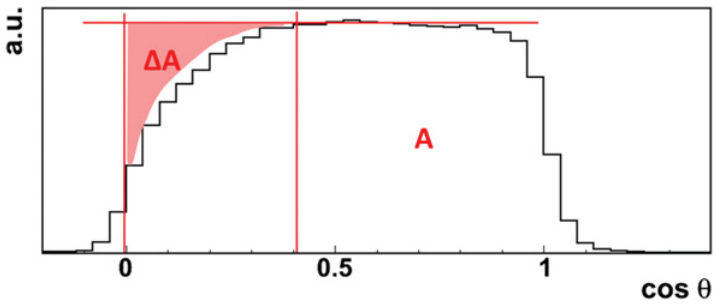

Figure 4. Angular distribution for ^{242}Pu. The FF loss inside the sample is visible at low cos θ values. By determining the integral of the distribution and ΔA (the missing part of the distribution) one can obtain the sample loss.

correspond to fragments emitted in the forward direction. The angular distribution obtained is shown in Figure 4. The degradation due to FF stopped inside the sample is visible at low cos θ values. To determine the total number of emitted FF (N_{cos}), one would do:

$$N_{cos} = A + \Delta A \tag{1}$$

with A being the integral of the cosinus distribution and ΔA the missing part related with the thickness of the sample. To extract the sample loss it is needed to consider the anode PH distribution (N_{PH}) and extrapolate down to 0 (ΔN_{PH}) to account for FF emitted but not detected due to the high electronic threshold requested not to trigger α events. The experimental efficiency due to sample loss (ϵ_{exp}) will be calculated as:

$$\epsilon_{\text{exp}} = \frac{N_{PH} + \Delta N_{PH}}{N_{cos}} = \frac{N_{2\pi}}{N_{cos}} \cdot \tag{2}$$

By performing this analysis for the two isotopes, we have obtained an ϵ_{exp} of $97 \pm 1\%$ for the ^{242}Pu and of $93 \pm 1\%$ for the ^{240}Pu. However, one would expect that the thicker sample has more loss than the thinner one. A careful look at Figure 2 shows that the preamplifiers, due to the high α-activity, were not completely discharged when the FF event occurred. The consequence is that neither the energy collected nor the angle detected will be the correct ones, even though the information that a FF has happened is correct. This effect is strongly related with the α-activity of the sample, the stronger this value the higher is the effect.

3.2.2 Improving signal rise time: P10 vs CH_4 as counting gas

By assuming that in our experimental system the preamplifiers are fast enough, the only way to verify the behaviour explained in the previous section would be to change the ionizing gas to one with much higher electron drift velocity. Hence, we have choosen CH_4 as it has a higher drift velocity than P10 [5]. Figure 5 presents in the left side a typical grid signal obtained with P10 for ^{240}Pu and on the right side with CH_4. The rise time of the signals is around 0.20 μs for the P10 case and 0.077 μs for CH_4. In the figure, it is possible to appreciate that with pure methane the α particle signals are well discriminated and the preamplifier is able to discharge almost completely before the next signal comes. In addition, the FF signal itself will have less probability to be piled-up within the rise time.

The analysis gives a preliminary ϵ_{exp} of $98.2 \pm 1\%$ for ^{242}Pu and $99.3 \pm 1\%$ for ^{240}Pu. As we see, the proportionality between sample thickness and sample loss is maintained.

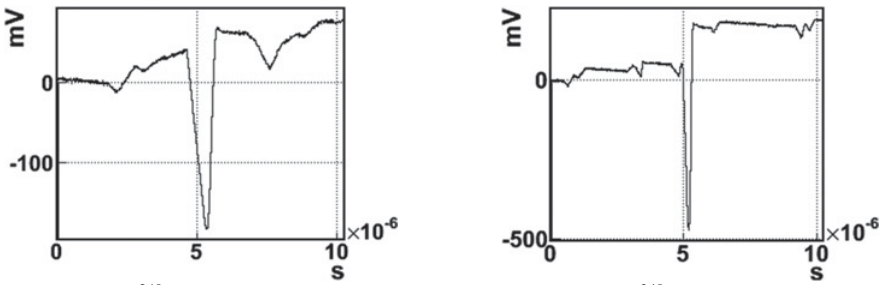

(a) ^{240}Pu with P10 (b) ^{240}Pu with CH_4

Figure 5. Grid signals obtained with ^{240}Pu using either P10 (left) or CH_4 (right). A big improvement is seen in the signal taken with CH_4, being able to discriminate between close by α particles.

3.2.3 Results on the sample efficiency

To verify the efficiency results obtained with the CH_4 gas, a theoretical calculation using SRIM [6] stopping power ranges and GEANT4 simulations [7] have been done. A brief explanation of the two methods is given.

Theoretical calculation:

The calculation has been done as presented in Ref. [3]. Properties for two typical FF have been used. The loss inside the sample can be calculated as:

$$\Delta_{\text{sample}} = \frac{t}{2R_{\text{sample}}} = \frac{t}{2}\sum_i \frac{W_i}{R_i} \tag{3}$$

with t as the thickness of the sample, R_i the range of isotope i and W_i the weight fraction of isotope i in the sample.

GEANT4:

Simulations with GEANT4 have been performed with a FF kinetic energy distribution obtained with the GEF code [8]. Those simulations are in an early stage but it is possible for us to extract already the amount of FF stopped in the samples.

Table 2 summarizes the results obtained using the 4 different methods: experimental using P10 as counting gas, experimental using CH_4, theoretical calculation and GEANT4 simulations. By changing the counting gas inside the TFGIC, it was possible to overcome almost completely the effect of the loss of information due to an incomplete discharge of the preamplifiers caused by the α pile-up. If we extrapolate this result, assuming the use of an even faster gas (in terms of drift velocity of the electrons) and ideal preamplifiers, we could experimentally verify the theoretical value. Therefore, the latter will be the one used for the SF half-life calculation.

4. Spontaneous fission half-life

The SF half-life has been calculated using:

$$T_{1/2,SF} = \frac{\%^j\text{Pu}}{\text{A}_j}\frac{1}{\left(\frac{C_{SF}}{t\cdot\epsilon_j\cdot\ln 2\cdot m_{\text{Pu}}\cdot N_A} - \sum_i^n \frac{\%^i\text{Pu}}{\text{A}_i\cdot T_{1/2,SF}(i)}\right)} \tag{4}$$

Table 2. Summary on the sample efficiency (ϵ) results by using different methods. Results of CH_4 and GEANT4 are preliminary.

	Experiment		Theory	GEANT4
	P10	CH_4		
^{240}Pu	$93 \pm 1\%$	$99.3 \pm 1.0\%$	99.7%	99.2%
^{242}Pu	$97 \pm 1\%$	$98.2 \pm 1.0\%$	98.1%	97.4%

Table 3. Summary of the spontaneous fission half-life ($T_{1/2,SF}$) for ^{240,242}Pu. The weighted average of literature values presented by Ref. [9] is shown as well.

$T_{1/2,SF}$ (y)	^{240}Pu	^{242}Pu
Holden (2000) [9]	$1.14 \times 10^{11}(0.9\%)$	$6.77 \times 10^{10}(1.0\%)$
This experiment (preliminary)	$1.146 \times 10^{11}(1.0\%)$	$6.745 \times 10^{10}(1.2\%)$

where $\%^j$Pu is the purity of the sample, A_j its atomic mass, C_{SF} are the counts detected, ϵ_j is the sample efficiency, m_{Pu} is the sample mass, N_A the Avogadro's number and $\sum_i^n \frac{\%^i\mathrm{Pu}}{A_i \cdot T_{1/2,SF}(i)}$ the contribution from the other isotopes contained in the sample.

Several measurements have been performed with each sample. Table 3 presents the weighted average of all measurements. The main contribution to the uncertainty is the efficiency and the sample mass. In addition, the weighted average of a subset of literature data from Ref. [9] is also given.

5. Results and conclusions

The need for improved neutron-induced fission cross sections of ^{240,242}Pu in the fast neutron spectrum range required a complete study of the behaviour of TFGIC with samples of high α-activity by using digital electronics. For the first time, we were able to correlate a degradation of the cosinus distribution with the number of α-particles piled-up in the time frame were we recorded the signal. By changing the counting gas from P10 to CH_4 we were able to solve almost completely the issue and cross check the efficiency that one can obtain using theoretical calculations and Monte Carlo codes with experimental values. Finally, the SF half-lives of both ^{240,242}Pu have been remeasured lowering the overall uncertainty (see Table 3).

References

[1] M. Salvatores, NEA/WPEC-26, OECD (2008)
[2] G. Sibbens et al., J. Rad. Nucl. Chem. in press (2013)
[3] C. Budtz-Jørgensen, H.-H. Knitter, Nucl. Sci. Eng. **86**, 10–21 (1984)
[4] A. Al-Adili et al., Nucl. Instr. and Meth. in Phys. Res. **A671** 103–107 (2012)
[5] G.F. Knoll, Radiation detection and measurement. 3rd edition. (2000) p. 133
[6] http://www.srim.org
[7] http://geant4.web.cern.ch/geant4/
[8] K.H. Schmidt, B. Jurado, GEF-code version 2.7
[9] N.E. Holden, D.C. Hoffman, Pure Appl. Chem. **72**, 1525–1562 (2000)